Artículo de investigación

Evidence of mixing and magmatic contamination in the lava of Tarum area, southwestern Gilan province (Iran)

Evidencia de mezcla y contaminación magmática en la lava del área de Tarum, provincia sudoeste de Gilan (Irán)

Evidência de mistura e contaminação magmática na lava da área de Tarum, sudoeste da província de Gilan (Irã)

Recibido: 20 de septiembre de 2018. Aceptado: 11 de octubre de 2018

Written by:
Fatemeh Ghotb-Tahriri[1]
Mohammad-Ali Arian*[1]
Shahrooz Haghnazar[2]
Mohsen Porkermani[1]
[1]*Department of geology, faculty of science, North Tehran Branch, Islamic Azad University, Tehran, Iran*
[2]*Department of geology, faculty of science, Lahijan Branch, Islamic Azad University, Lahijan, Iran*
*Email: m_arian@iau-tnb.ac.ir

Abstract

The studied area is located in the high altitudes of Tarum region on the Alborz mountainous area, southwestern Gilan province, IranAccording to the tectonic- sedimentology aspect, the region has been located on Western Alborz- Azerbaijan zone. The igneous rocks of the area are generally pyroclastic units and the lavas ages belong to Eocene to Oligocene. Lavas are basalt, andesite, trachyandesite, dacite and rhyolite. Pyroclastic rocks are tuffs (lithic crystal tuff, halo-lithic tuff, sandy tuff, clay tuff and tuffit), ignimbrite, breccia, scoria and pumice. Rhythmic lava layering based on its composition represents a diffraction in a magma chamber. Results of microscopic studies (e.g. nonhomogeneous mineral accumulation, selective mineral alteration, erosion and opacification of mineral margins, Serration boundaries among phenocrysts, sieve texture, opacity margin and globule faces, Oscillatory zoning in clinopyroxene, inclusion zones in plagioclase, two generation types of plagioclase crystals and needle shape apatite) reveal magmatic evaluation including Crystal fractionation, magma mixing and magmatic contamination in the rocks. The trend for comparative pattern for basic, intermediate and acidic samples are parallel and it shows the trend for the continental crust representing the similar source among the samples and crust contamination. The source magma these rocks have been influenced by AFC (Assimilation

Resumen

El área estudiada se ubica en las altitudes elevadas de la región de Tarum en la zona montañosa de Alborz, en el sudoeste de la provincia de Gilan, Irán. Según el aspecto tectónico-sedimentológico, la región se encuentra en la zona occidental de Alborz-Azerbaiyán. Las rocas ígneas de la zona son generalmente unidades piroclásticas y las edades de las lavas pertenecen al Eoceno y al Oligoceno. Las lavas son basalto, andesita, traquyandesita, dacita y riolita. Las rocas piroclásticas son tobas (toba de cristal lítica, toba halolítica, toba de arena, toba de arcilla y toba), ignimbrita, brecha, escoria y piedra pómez. La estratificación de lava rítmica basada en su composición representa una difracción en una cámara de magma. Resultados de estudios microscópicos (por ejemplo, acumulación de minerales no homogéneos, alteración selectiva de minerales, erosión y opacificación de márgenes minerales, límites de sangrado entre fenocristales, textura de tamiz, margen de opacidad y caras de glóbulos, zonificación oscilatoria en clinopiroxeno, zonas de inclusión en plagioclasa, tipos de plagioclasa de dos generaciones Los cristales y la apatita en forma de aguja) revelan una evaluación magmática que incluye fraccionamiento de cristales, mezcla de magma y contaminación magmática en las rocas. La tendencia del patrón comparativo para muestras básicas, intermedias y ácidas es paralela y muestra la tendencia de la

Fractional Crystallization) and FC (Fractional Crystallization) processes; hence, the geochemical properties are away from its source.

Keywords: Tarum, Lava, pyroclastic, magma combination and mixing, magma contamination, fractionation, continental crust.

corteza continental que representa la fuente similar entre las muestras y la contaminación de la corteza. La fuente magma de estas rocas ha sido influenciada por los procesos de AFC (cristalización fraccionada por asimilación) y FC (cristalización fraccionada); Por lo tanto, las propiedades geoquímicas están lejos de su origen.

Palabras claves: Tarum, lava, piroclástico, combinación y mezcla de magma, contaminación de magma, fraccionamiento, corteza continental.

Resumo

A área estudada está localizada nas altas altitudes da região de Tarum, na região montanhosa de Alborz, sudoeste da província de Gilan, Irã. De acordo com o aspecto tectônico-sedimentológico, a região foi localizada na zona oeste de Alborz-Azerbaijão. As rochas ígneas da área são geralmente unidades piroclásticas e as idades das lavas pertencem ao Eoceno ao Oligoceno. Lavas são basalto, andesito, traquidandesita, dacito e riolito. As rochas piroclásticas são tufos (tufo de cristal lítico, tufo halo-lítico, tufo arenoso, tufo de barro e tuffit), ignimbrito, brecha, escória e pedra-pomes. Camadas de lava rítmica baseadas em sua composição representam uma difração em uma câmara de magma. Resultados de estudos microscópicos (ex: acúmulo mineral não homogêneo, alteração mineral seletiva, erosão e opacificação de margens minerais, limites de Serration entre fenocristais, textura de peneira, margem de opacidade e faces de glóbulos, zoneamento oscilatório em clinopiroxênio, zonas de inclusão em plagioclásio, dois tipos de plagioclásio cristais e apatita em forma de agulha) revelam uma avaliação magmática incluindo fracionamento de Cristal, mistura de magma e contaminação magmática nas rochas. A tendência do padrão comparativo para amostras básicas, intermediárias e ácidas é paralela e mostra a tendência da crosta continental representar a fonte similar entre as amostras e a contaminação da crosta. O magma fonte dessas rochas tem sido influenciado pelos processos AFC (Cristalização Fracionada de Assimilação) e FC (Cristalização Fracionada); Portanto, as propriedades geoquímicas estão longe de sua origem.

Palavras-chave: Tarum, Lava, piroclástico, combinação e mistura de magma, contaminação por magma, fracionamento, crosta continental.

Introduction

The Study area is located in Tarum mountain, Alborz mountainous area, SW Gilan province, Iran. It is located between Eastern longitude of 49o00’ to 49o15’ and Northern latitude of 36o30’ to 36o45’ in the southern part of 1:100k geological map of Rudbar.

Based on the Iran geological zonation classification for Alborzand its structural units in the east and west, the area belongs to Tarum-Hashtjin zone (Nabavi, 1976). Based on 1:100K geological map of Rudbar, semi deep igneous rocks (as a dyke, sill, or dome) and deep massive igneous rocks with different compositions have been penetrated and located within lower cretaceous limy-marl rocks, volcanic rocks and tertiary pyroclastic units (especially Eocene to Oligocene). The geological properties of this area have been significantly influenced by its tectonic location which is in the collision of Iran and Turan plate in one hand and it is on the margin of active continental plate of Alborz. Turan and Iran plates got close together as soon as paleo Tethys oceanic surface appeared and subduction of the oceanic crust under the southern part of Turan plate gave rise to a complete collision of these two plates in the late Triassic (Alavi, 1996). Based on (Alavi, 1996), Tarum mountainous area which is located on Alborz margins as a magmatic arc has been influenced by tectonic process and movements in late Cretaceous. These movements might have

been caused by an oceanic crust subduction toward the Alborz continental crust in late cretaceous-Paleocene. Upper calk alkaline volcanism in western-central Alborz started under the subduction happened in Paleocene-Eocene (mostly in middle to upper Eocene). Orogeny activities in Miocene has been intensified by forming an alkaline magma confirming tensile activities during the collision. Upper Eocene and Oligocene magmatism in Tarummountains resulted in increasing geothermal degree as well as injecting shallow intrusive rocks with high sulfate hydrothermal solution which gave rise to wide alteration (Peyrowan, 2002). The main purpose of this paper is to study the mixing and magmatic contamination evidence via petrographical, lithological and geochemical studies and magma evaluation.

Literature review

Geological Survey of Iran (GSI) carried out a research entitled ''prospecting gold and systematic geochemical exploration in Kohyan'' in Tarum mountainous areas (especially in Kahia, Gohar and Kohyan villages) (Abedian et al, 2009). Moayyed believed that the volcanoplutonic belt of Tarum as well as copper mineralization has been formed by the subduction process (Moayyed, 1991). Also, several master and PhD thesis have studies minerals and deposits in Tarum area (e.g. 1:100K geological map of Tarum(Amini, 2000), 1:250k geological map of Zanjan(Eftekharnejad, 1969), 1:100K geological map of Rudbar(Nazari, 1998), systematic geochemical exploration of Abhar (1:100K map) (Abedian et al, 2004).

General geology

Based on the geological field trip and 1:100K geological map of Rudbar (Figure 1), the dominant outcrops of the area include Neogene red formation (contains gypsum) and conglomerate, tertiary (mostly Eocene to Oligocene) volcanic units, pyroclastic and granitoid units (with the direction of NW-SE). These units (from the oldest to the youngest are) Etv, Ev, Et, Eta, Et2, Ev1, Et1,G1andG2 which are the sequence of basic lavas, basalt-andesite lavas, trachyandesite, acidic lavas of dacite-rhyolite and pyroclastic units including tuffs (lithic crystal tuff, hailolithic tuff, sandy tuff, clay tuff and tuffit), ignimbrite, breccia, scoria, pumice, granitoid and aplite.

Lava units was deposited in different erosion phase as a basic to intermediate lavas as well as acidic and volcanoclastic lavas like tuff, ignimbrite and breccia (figure 2A-1). In a macroscopic studies, lithic crystal tuff units have lithic fragments with a bright color about 5 to 10cm.They are look more acidic and brighter than other parts (Figure 2A-3). A good layering of tuff sandstone has been appeared after the lithic crystal tuff layer (Figure 2A-4). These changes (from lithic crystal tuffs to sandy tuff) can show volcanic conditions in the area (Figure 2A-2).

Large amount of ignimbrite has an outcrop of around 65m in this area (Figure 2A-5). Lava units are usually associated with rhythmic layering and dark lavas with Columnar structure are seen in the bottom units and lighter lavas have been placed on the upper parts (Figure 2A-6). It seems that a magma chamber fractioned in the chamber was responsible for this stratigraphy. A lot of Enclaves have been formed in these lava units. These Enclaves can be responsible for magmatic contamination.

Material and method

Sampling process has been carried to study the volcanic rocks of the region after studying the distribution of rock data and their field relationship. Different samples were chosen for microscopic studies. After the microscopic studies, 23 samples have been sent to a laboratory for Lithium Borate Fusion, ICP-OES and ICP-MS analysis for analysis of the main and rare elements. The results have been also analyzed and interpreted by IGPET2007 and GCD-KIT software. Based on the spider diagrams and the geochemical and tectonomagmatism interpretation on the major and rare elements in the magma which will be presented later in this paper the influence of the magma contamination and evaluation as well as the magma origin has been studied.

Discussion

Petrography

Following lava units can be recognized based on the petrographic analysis: 1st group: olivine basalts and basalts; 2nd group: andesite basalts and andesites; 3rdtrachyandesites; 4th group: dacites and rhyodacites; 5th group: rhyolites; 6th group: pyroclastics.

Olivine basalts and basalts: the texture is mostly porphyritic with microlitic and vesicular matrix, microporphyritic with fluidal microlitic matrix, porphyritic microlitic and amigdaloidal (Figure 2B-2).

The phenocrysts include olivine, augite, plagioclase (labradorite-bitonite type) and opaque. The matrix also includes plagioclase and augitemicrolite. Minor phase minerals include apatite and altered chlorite and calcite and opaque. Plagioclase are seen as two generations (phenocryst and microlite) (Figure 2B-1).

Basaltic andesites, andesites and pyroxene andesites: the texture is mostly hyaloporphyritic with glassy matrix, porphyritic, microlitic, microlitic porphyritic and glomeroporphyritic (Figure 2B-4). Phenocrysts include plagioclase (andesine, augite, biotite, amphibole, opaque, and some parts of exotic lithic fragments in the form of Xenolith in matrix. The matrix include dark and vacuolar glass, plagioclase phenocryst, pyroxene, biotite and opaque minerals. Plagioclase phenocrysts and pyroxene (Figure2B-3) are mostly altered, sieved and skeletal. Quartz and apatite are seen in plagioclase. Biotite and augite have been changed to reactional margins and embayment around the phenocrysts. Miner phase minerals are opaque, talc, epidote, and secondary minerals (mostly altered) are calcite, apatite, silica and chlorite.

Trachyandesites and quartz trachyandesites: the texture is mostly hyaloporphyritic with fluidal and glassy matrix, microlitic and trachytic. Phenocrysts are plagioclase (albite), orthoclase and sanidine, augite, biotite, amphibole, epidote (pistacite), quartz and opaque minerals. The matrix is dark glassy and vacuolar and it has been composed of microlitic feldspar, microphenocryst of quartz, feldspar, augite, epidote and opaque minerals (Figure 2B-5). Biotite has been placed in augitephenocryst in a form of poikilitic representing the fact that biotite crystallization has been performed in a first stage of the crystallization. Minor minerals are apatite, opaque, zircon, and secondary minerals of muscovite, calcite and chlorite.

Dacites and Rhyodacites: The texture is mostly porphyritic with microgranular matrix. Phenocrysts are plagioclase (albite-oligoclase), orthoclase and sanidine, quartz, biotite and opaque. The matrix has been made of glass, alkali feldspar and plagioclase. Plagioclase phenocrysts have been mostly altered and they show zoning and polysyntethic twinning. Alkali feldspar phenocrysts have been altered to clay minerals (sericite) and kaolinite. Minor phase minerals are chlorite, malachite and opaque distributed in the matrix (Figure 2B-6).

Rhyolites: the texture is mostly porphyritic with microgranular matrix. Phenocrysts are plagioclase (albite-oligoclase), quartz, orthoclase and sanidine. The matrix is composed of quartz and alkali feldspar crystals. Plagioclase and alkali feldspar phenocrystals have been entirely altered to clay minerals (Figure 2B-7). The Xenolithes are mostly granular in the lava units. The minerals include plagioclase, pyroxene, opaque, biotite and quartz. Minor phase minerals are zircon and opaque, and calcite is seen as a secondary mineral (Figure 2B-10).

Pyroclastics have been formed with porphyritic texture and fluidal and glassy matrix. The phenocrysts are plagioclase, alkali feldspar, pyroxene, biotite, and opaque. The matrix is a dark, fluidal glass with microphenocrystals of plagioclase, biotite, pyroxene, and quartz (Figure 2B-8). In the sandy tuff can be seen layering in matrix. Breccia samples have brecciated texture and altered and eroded and have got several lithic fragments (Figure 2B-9).

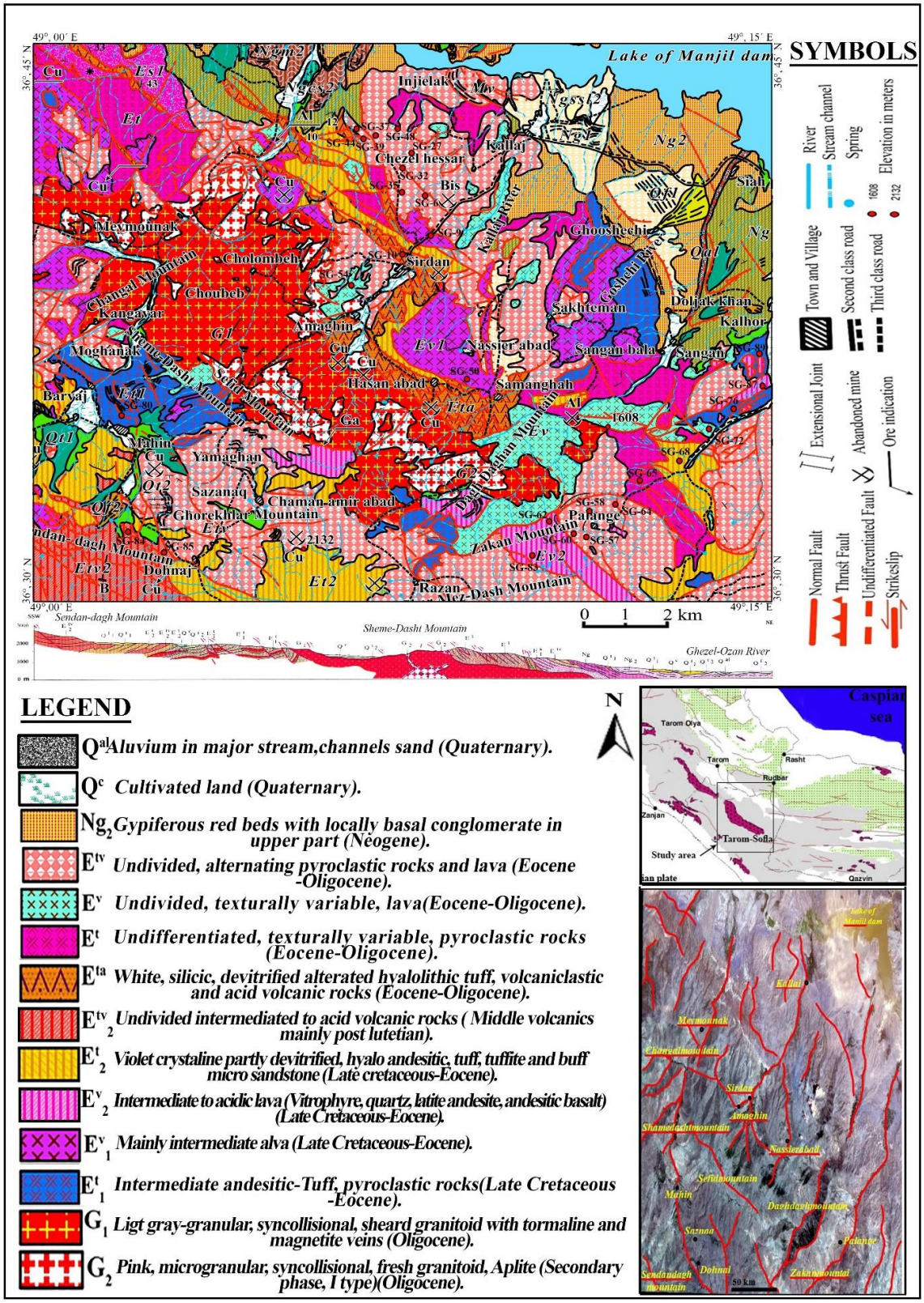

LEGEND

- Q^{al} *Aluvium in major stream,channels sand (Quaternary).*
- Q^{c} *Cultivated land (Quaternary).*
- Ng_2 *Gypiferous red beds with locally basal conglomerate in upper part (Neogene).*
- E^{tv} *Undivided, alternating pyroclastic rocks and lava (Eocene -Oligocene).*
- E^{v} *Undivided, texturally variable, lava(Eocene-Oligocene).*
- E^{t} *Undifferentiated, texturally variable, pyroclastic rocks (Eocene-Oligocene).*
- E^{ta} *White, silicic, devitrified alterated hyalolithic tuff, volcaniclastic and acid volcanic rocks (Eocene-Oligocene).*
- E^{tv}_2 *Undivided intermediated to acid volcanic rocks (Middle volcanics mainly post lutetian).*
- E^{t}_2 *Violet crystaline partly devitrified, hyalo andesitic, tuff, tuffite and buff micro sandstone (Late cretaceous-Eocene).*
- E^{v}_2 *Intermediate to acidic lava (Vitrophyre, quartz, latite andesite, andesitic basalt) (Late Cretaceous-Eocene).*
- E^{v}_1 *Mainly intermediate alva (Late Cretaceous-Eocene).*
- E^{t}_1 *Intermediate andesitic-Tuff, pyroclastic rocks(Late Cretaceous -Eocene).*
- G_1 *Ligt gray-granular, syncollisional, sheard granitoid with tormaline and magnetite veins (Oligocene).*
- G_2 *Pink, microgranular, syncollisional, fresh granitoid, Aplite (Secondary phase, I type)(Oligocene).*

Figure 1- Geological map of the study area (part of Rudbar 1:100K geological map (Nazari,1998)

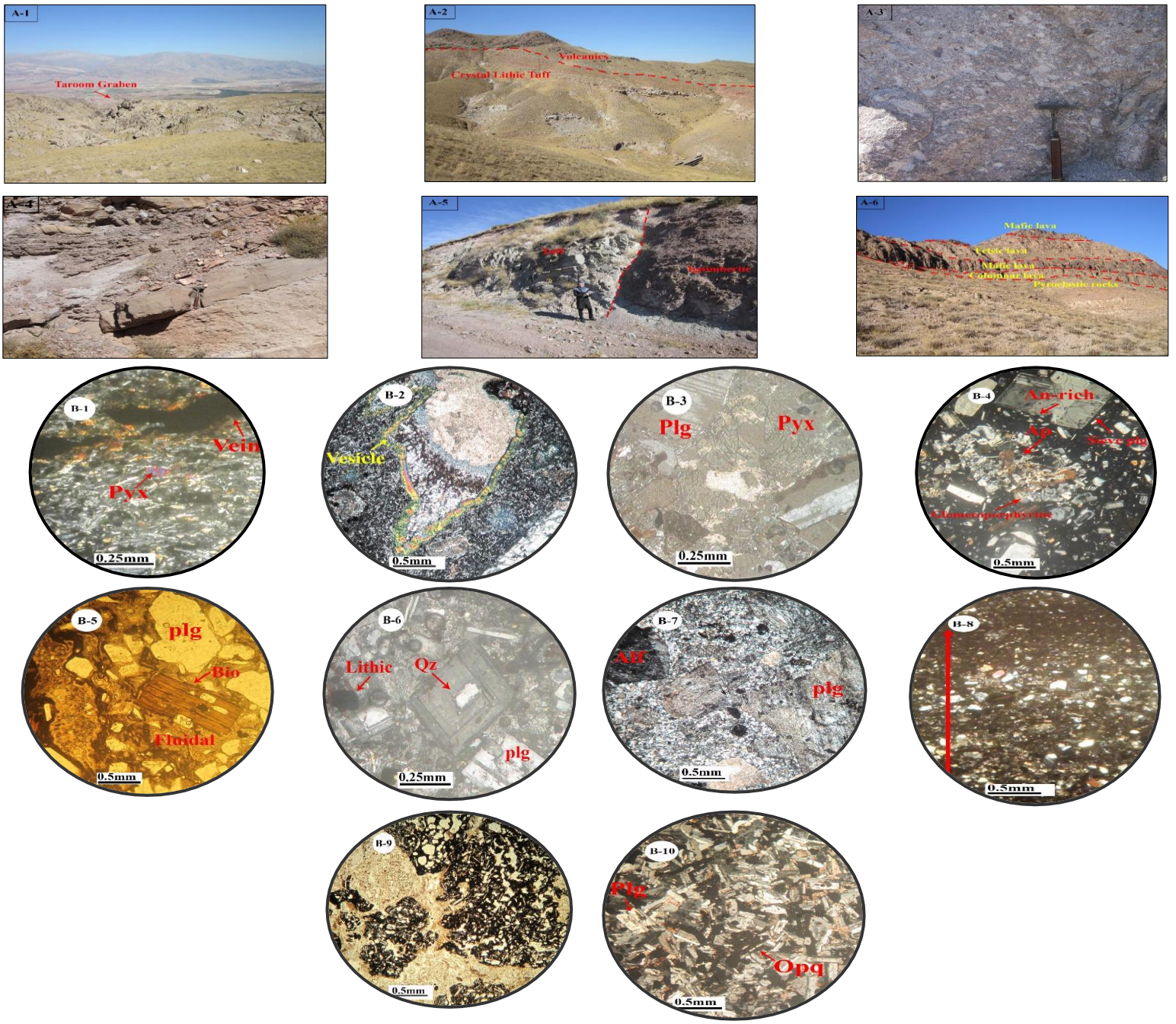

Figure 2- A1-2: pyroclastic and lava samples (the outcrops of Tuffaceous sandstone zone between two zone of lithic crystal tuff and lava (View to north). A-3: a view of lithic crystal tuff (View to south). A-4: a view of tuffy sandstone zone (view to north). A-5: a view of a contact between ignimbrite and tuffy units (view to south). A-6: a view of rhythmic and columnar structure of lava units (view to north). B-1: A microscopic image of plagioclase microlites, pyroxene and a vein which are being under alteration in olivine basalt (XPL-Magnification (M): 200x). B-2: A microscopic image of amigdaloidal texture in olivine andesite basalt (XPL- M:40x). B-3: Pyroxene phenocrystal with skeletal texture in an andesite basalt sample (XPL- M:200x). B-4: Plagioclase phenocrystal with sieve texture and glomeroporphyritic in andesite (XPL- M: 40x) . B-5: phenocrystals of biotite and plagioclase in a matrix consisted of microphenocrystals of plagioclase and biotite and fluidal glass in trachyandesite (PPL- M: 40x). B-6: phenocrystals and microphenocrystals of plagioclase and quartz in dacite and rhyodacite (XPL- M: 200x). B-7: Altered alkali feldspar and plagioclase phenocryst in rhyolite (XPL- M:40x). B-8: Sandy tuff with layering (XPL- M: 40x). B-9: Breccia sample with plenty of lithic fragments (XPL- M: 40x). B-10: Enclaves with granular texture and plagioclase, pyroxene and opaque minerals (XPL- M: 40x)

Geochemistry

The results of chemical analysis have been presented in tables 1, and 2. 54 major and rare

elements have been measured to assess and compile the geochemical properties of the lava.

In the diagram of Zr/TiO2 versus Nb/Y (Winchester, 1977), the samples have been placed on sub alkaline basalt, alkali basalt, andesite, trachyandesite, dacite and rhyodacite (Figure 3a). Based on FeO*/MgO versus TiO2, the collected samples have shown the calk alkaline and tholeiitic trend (Miyashiro, 1974; Khalifa et al, 2011) (Figure 3b).

Figure 4 shows the major and rare elements versus DI. Based on this figure, MgO, TiO2, CaO, Al2O3 and FeO show a decreasing trend while it has an increasing trend for K2O, Na2O, Th, Nb, and Ta. These phenomena might have happened because of magmatic fractionation and separating the minerals containing iron, magnesium, and titanium, opaque as well as olivine, augite, and plagioclase in the study area.

Different trends for the samples can outline the influence of magmatic contamination on the magma evaluation trend for the samples of the study area.

The charts described above can significantly show the rule of fractional crystallization within the magma evaluation. In the all charts, regular changes can be seen for basic to acidic samples (Ghotb, 2017). Based on Figures 5a and 5b (rare earth elements pattern for basic and intermediate samples (Sun and McDonough,1989) more concentration can be seen for Cs, Ba, Pb, K, Sr, and u and less concentration is seen for Y, Zr, P, Nb and Ta. The anomalous data and low values of Nb/U and Ce/Pb as well as high values of Th/Nb and Ba/Zr can be related to the crustal intervention on the magmatic evaluation (Taylor, 1985). In the REE patterns, LREE to HREE show a significant concentration. Two factors can be responsible for this concentration: (1) LREEs are partly more incompatible than HREEs; hence, LREE might have been placed during the magma evaluation process in transformed rocks in area (Li et al, 2016; Dostal, 2017; Winter, 2001) (2) the genesis might have been related to subduction areas or crustal contamination (Winter, 2001; Khalatbari, 2016) (figure 5d). Based on the pattern of average elements chondrite normalized, the studied samples show a close relationship with the trend of continental crust (figure 5c).

Magma mixing and contamination

Microscopic studies (on thin sections) revealed significant evidence on the fact that magma mixing and contamination had a significant rule on forming the rock units in the area. The most important texture and minerals evidence are:

1. Although olivine has been entirely altered throughout the samples, augite next to olivine has little or no alteration or activated margins (Wilshire et al, 1991; Koyaguchi, 1991; Wright, 1996).
2. Significant difference on the phenocryst based on the selective alteration
3. Opacitic margins in hornblende and biotite.
4. Serration edge and highly eroded minerals and henocrysts which cause an embayment structure.
5. Zonal structure in augite and plagioclase phenocryst.
6. Zones with fluid inclusion and crystalline absorption in plagioclase (Shelly, 1993; Thomas, 1997).
7. Excising two generations of plagioclase crystals in one sample.
8. Needle shape apatite as an inclusion.
9. Globule shaped faces.
10. Existing Exotic lithic fragments or Xenoliths in the host rock.
11. Sieve texture in plagioclase and augite.

Low value of Nb/Y and high value of Rb/Y (figure 5e) confirms the crustal contamination of the samples in the depleted mantle (Zhao et al, 2007; Kepezhinskas et al, 1996; Cai et al, 2014). Based on the diagram of Th/Yb versus Ta/Yb, the samples have been mostly influenced by FC and AFC. Also the positive concentration of Th/Yb versus the constant value of Ta/Yb shows the crustal contamination to the upper crust (figure 5f). Based on Th/Yb versus Ta/Ybdagram(Pearce,1983; Zarasvandi et al, 2015; Kheirkhah, 2013; Kamali et al, 2011), the samples have been located on the active continental margins and they follow crustal contamination vector (C) (figure 5g).

Based on the diagram of Nb/Th versus Ti/Yb(Feigenson, 1996; Hofmann 1996), the samples might have been derived from Middle Crust (MC) of intermediate compositions. There is also a close geochemical relationship between the samples and intermediate to basic samples. Therefore, the samples can be considered as a product of crustal contamination during the

fractional crystallization originated from basaltic magma (Figure 5h).

Table 1- Results of major and based elements concentration by ICP and Lithium Borate Fusion method (An: Andesite; Trcy An: Trachy Andesite; Ba: Basalt; Q: Quartz; Ol: Olivine; Pyx: Pyroxene)

Sample #	*SG-57*	*SG-72*	*SG-85*	*SG-54*	*SG-65*	*SG-89*	*SG-62*	*SG-48*	*SG-76*	*SG-35*	*SG-32*	*SG-39*
Sample name	***Ol-Basalt***	***Ol-Basaltic andesite***	***An***	***Tracy An***	***Q-Trachy andesite***	***An***	***Tracy An***	***Tracy An***	***Pyroxene-andesite***	***Q-Trachy andesite***	***Pyroxene-andesite***	***Tracy An***
N	31′53.˚367"	34′6.3"˚36	31′33.7˚36"	38′17.1˚36"	32′30.4˚36"	35′7.5"˚36	31′53.8˚36"	42′22.5˚36"	33′57.6˚36"	41′30.2˚36"	41′51.7˚36"	42′8.˚362"
E	17′31"˚49	20′28.5˚49"	04′34"˚49	10′26.5˚49"	18′17.5˚49"	21′46.7˚49"	17′30.5˚49"	12′26.6˚49"	20′27.2˚49"	12′3.3"˚49	12′26.8˚49"	12′3.˚499"
						Wt%						
SiO_2	49.33	50.44	52.27	52.83	57.81	59.82	60.58	62.19	62.45	62.63	62.69	63.24
Al_2O_3	17.64	15.61	14.68	17.8	16.3	16.66	17.19	15.42	16.09	15.63	15.96	15.84
CaO	9.99	8.68	9.53	6.58	2.94	3.48	1.64	5.13	4.35	3.74	4.14	4.14
Fe_2O_3	2.77	2.48	2.35	2.54	2.47	2.15	2.25	2.05	2.07	1.96	2.02	2.05
FeO	6.48	4.4	4.54	4.61	5.17	2.83	3.15	1.47	2.68	1.85	1.84	1.89
K_2O	1.25	2.33	3.14	3.77	1.23	3.14	3.14	2.21	1.6	3.49	1.94	2.04
MgO	4.96	2.57	4.38	2.9	2.92	2.62	1.74	1.19	1.85	1.82	1.61	1.55
MnO	0.3	0.14	0.21	0.18	0.19	0.09	0.1	0.07	0.12	0.08	0.18	0.1
Na_2O	3.14	2.83	2.17	3.61	5.71	2.91	6.47	3.08	4.68	3.6	4.25	4.44
P_2O_5	0.22	0.31	0.24	0.31	0.22	0.29	0.17	0.16	0.18	0.14	0.17	0.17
TiO_2	1.27	0.98	0.85	1.04	0.97	0.65	0.75	0.55	0.57	0.46	0.52	0.55
$Mg^{\#}$	50	40.64	54	42.51	41.37	49.61	37.39	38.6	44.5	47.36	45.05	42.2
LOI	1.76	8.62	4.58	3.11	3.45	4.79	2.35	5.99	3.44	3.8	4.21	3.55
Total	99.84	99.88	99.9	99.8	99.96	99.75	99.89	99.68	99.82	99.41	99.74	99.78

Sample name	***An***	***An***	***An***	***Tracy An***	***Tracy An***	***Dacite***	***Q-Trachy andesite***	***Q-Trachy andesite***	***Q-Trachy andesite***	***Tracy An***	***Rhyolite***
N	41'55.˚364"	42'8"˚36	41'20˚36"	39'23.˚369"	30'53"˚36	42'9.˚363"	31'40"˚36	31'55.3"˚36	31'53.8"˚36	33'11.9"˚36	35'4.8 "˚36
E	12'28.˚491"	12'5.˚491"	12'50˚49"	11'50.˚496"	16'42"˚49	12'2.˚496"	17'42"˚49	17'30.4"˚49	17'30"˚49	19'10.3"˚49	21'47.1"˚49
						Wt%					
SiO_2	63.36	63.41	63.47	64.73	67.09	67.19	68.89	69.78	70.42	72.5	73.13
Al_2O_3	15.69	15.73	16.35	16.36	15.2	15.47	15.44	15.22	13.89	13.87	12.95
CaO	3.97	2.85	4.29	3.48	1.8	3.07	1.3	1.17	1.79	0.85	1.37
Fe_2O_3	2.01	2.08	2.05	2.01	2.04	1.99	1.93	1.91	1.83	1.85	1.82

FeO	1.77	1.98	1.72	1.92	0.76	1.92	0.73	0.57	0.036	1.62	1.51
K_2O	1.63	3.97	3.88	4.01	5.61	4.51	4.08	3.86	5.44	5.19	4.37
MgO	1.75	2.02	0.68	0.76	0.76	0.49	1.07	0.61	0.48	0.28	0.23
MnO	0.1	0.13	0.13	0.05	0.09	0.03	0.11	0.09	0.14	0.03	0.02
Na_2O	4.56	3.54	4.29	3.86	2.53	3.41	4.26	4.98	3.56	3.39	3.79
P_2O_5	0.17	0.16	0.17	0.14	0.05	0.16	0.08	0.08	0.04	0.04	0.04
TiO_2	0.51	0.58	0.55	0.51	0.54	0.49	0.43	0.41	0.33	0.35	0.32
$Mg^{\#}$	46.7	48.54	24.61	26.08	33.3	19.04	43.3	32.6	32.35	24.001	21.36
LOI	4.1	3.17	2.1	1.81	3.32	0.91	1.51	1.17	1.96	1.55	2.01
Total	99.82	99.84	99.88	99.86	99.88	99.86	99.92	99.92	99.92	99.86	99.91

Table 2- Results of rare earth elements concentration by ICP method (An: Andesite; Trcy An: Trachy Andesite; Ba: Basalt; Q: Quartz; Ol: Olivine; Pyx: Pyroxene)

Sample #	*SG-57*	*SG-72*	*SG-85*	*SG-54*	*SG-65*	*SG-89*	*SG-62*	*SG-48*	*SG-76*	*SG-35*	*SG-32*	*SG-39*
Sample name	***Ol-Basalt***	***Ol-Basaltic andesite***	***An***	***Tracy An***	***Q-Trachy andesite***	***An***	***Tracy An***	***Tracy An***	***Pyroxene-andesite***	***Q-Trachy andesite***	***Pyroxene-andesite***	***Tracy An***
						ppm						
Ba	653	625	567	917	365	1059	983	945	799	851	924	832
Ce	40	51	47	56	45	65	61	54	53	53	63	57
Co	29.5	22.5	22.5	18.5	19.9	7.6	10.3	8.5	10.2	7.4	7.5	7.6
Cr	16	55	97	101	22	7	8	7	12	11	9	11
Cu	100	27	45	60	5	19	4	9	35	33	29	22
Cs	3.5	5.7	1.7	4.6	1.1	4.8	1.3	7.3	6.2	3.8	29.7	10.7
Dy	3.61	3.96	4.06	3.73	3.36	4.01	3.59	3.04	3.1	2.45	3.13	3.22
Er	1.94	2.28	2.34	2.16	1.81	2.3	1.77	1.81	1.8	1.34	1.54	1.69
Eu	1.43	1.3	1.39	1.57	1.23	1.79	1.49	1.24	1.21	1.06	1.24	1.27
Fe	7.51	5.29	5.41	5.94	6.26	3.38	3.73	2.49	2.87	2.63	2.61	2.65
Gd	3.35	3.62	3.71	3.58	3.1	4.15	3.15	3.01	3.22	2.4	3.07	3.15
Hf	1.76	3.32	3.09	1.18	1.89	4.33	1.52	2.13	2.57	1.78	2.47	2.27
K	10965	19230	26685	30959	10626	26022	25821	18421	13745	28617	16168	16619
La	16	23	25	29	20	33	28	30	29	29	33	31
Lu	0.23	0.31	0.34	0.28	0.21	0.36	0.2	0.25	0.27	0.22	0.23	0.24
Mn	1841	890	1325	1092	1180	549	623	473	750	489	1096	609
Nb	7.2	11.3	9.6	12.8	6.4	12.8	10.7	10.4	10.9	10.3	11.1	11.1
Nd	14.1	19.1	18.3	19.1	14.9	25.4	20.1	18.7	18.5	15	18.9	19.1
Ni	13	19	25	19	9	<1	<1	1	3	3	2	2
P	1114	1449	1221	1619	1175	1503	908	827	886	730	887	864
Pb	13	5	9	11	15	9	23	4	9	8	9	10

Pr	1.9	3.54	3.2	3.6	2.25	5.36	4.11	3.93	3.77	3.1	4.14	4.03
Rb	24	55	75	97	32	66	66	56	81	81	50	50
Sc	26.9	16.4	27.3	18.8	23.1	7.8	9.8	7.2	8.7	6.5	7.5	7.7
Sm	3.9	4.65	4.65	4.57	3.72	5.55	4.54	4.15	4.11	3.44	4.18	4.23
Sr	554.6	442.1	532.4	635.9	217.4	377	380.3	1331.4	531.5	480.4	741.9	581.3
Ta	0.67	0.93	0.8	0.97	0.62	0.99	0.92	0.82	0.85	0.91	0.96	0.86
Tb	0.65	0.68	0.67	0.63	0.61	0.7	0.58	0.54	0.56	0.45	0.53	0.53
Th	1.1	5.82	5.1	6.18	2.13	8.38	4.45	8.49	7.71	7.99	8.75	8.98
Ti	9104	6153	5966	7405	6980	4719	5203	3599	4028	3140	3644	3818
Tm	0.36	0.41	0.44	0.38	0.34	0.42	0.32	0.34	0.37	0.3	0.33	0.34
U	0.5	1.8	1.7	1.5	0.7	2.3	2.01	1.66	2.6	2.3	2.5	2.5
V	288	166	204	201	113	73	109	70	90	64	71	75
Y	16.9	18.9	22	18.8	14	19.8	15.7	16.2	16	12.8	15.7	16.1
Yb	1.7	2	2.1	1.9	1.6	2.2	1.5	1.7	1.7	1.4	1.5	1.6
Zn	162	80	73	105	107	79	122	43	65	73	72	61
Zr	63	133	121	21	24	172	33	61	82	47	70	64

Table 2. Continue

Sample#	*SG-27*	*SG-37*	*SG-6*	*SG-9*	*SG-83*	*SG-44*	*SG-58*	*SG-64*	*SG-60*	*SG-68*	*SG-87*
Sample name	***An***	***An***	***An***	***Tracy An***	***Tracy An***	***Dacite***	***Q-Trachy andesite***	***Q-Trachy andesite***	***Q-Trachy andesite***	***Tracy An***	***Rhyolite***
						ppm					
Ba	757	825	786	755	829	864	632	756	480	940	348
Ce	57	54	50	45	52	49	67	67	67	57	67
Co	7.2	8.3	8	8	3.9	5.1	3.1	2	1.4	1.6	<1
Cr	8	10	9	8	8	10	7	7	7	6	6
Cu	16	43	16	8	6	17	6	9	7	15	9
Cs	28.2	3	3.6	3.8	4.3	9.7	4.5	3.4	1.8	3.5	2.3
Dy	3.08	2.82	2.44	2.12	3.32	2.77	3.3	2.99	4.33	3.03	3.36
Er	1.69	1.51	1.41	1.13	2.1	1.41	2	1.85	2.92	1.94	2.19
Eu	1.11	1.1	0.96	0.92	0.98	1.02	1.08	1.06	0.78	0.78	0.66
Fe	2.59	2.71	2.65	2.67	2.07	2.71	1.97	1.82	1.37	1.29	1.25
Gd	3.01	2.77	2.36	2.07	2.87	2.58	3.08	2.83	3.71	2.86	3.5
Hf	2.48	1.85	2.2	1.87	2.13	2.11	3.69	3.41	2.43	3.34	2.57
K	13347	32402	30860	31537	46040	35802	33545	30956	44405	41334	36404
La	33	29	26	25	31	25	40	38	37	32	39
Lu	0.24	0.22	0.21	0.17	0.34	0.19	0.29	0.29	0.43	0.34	0.42
Mn	609	825	834	322	553	207	676	553	839	213	130

Nb	10.5	9.7	11	9.9	20.8	11.4	11.4	11.8	20	15	19.7
Nd	18.7	16.7	14.2	12.9	17.1	16.5	19.3	18.4	22.5	17.3	22.8
Ni	2	3	4	2	1	2	<1	<1	<1	<1	<1
P	838	791	853	736	310	793	453	421	247	260	244
Pb	11	6	19	6	27	14	11	7	39	18	21
Pr	3.88	3.44	2.71	2.45	3.67	3.24	4.43	4.19	5.32	4.02	5.51
Rb	49	97	89	91	129	108	105	90	140	132	113
Sc	7.2	7.8	7.1	5.8	5.8	5.5	5.3	4.8	4.4	3.3	4
Sm	3.89	3.74	3	2.66	3.75	3.37	3.73	3.6	4.6	3.41	4.45
Sr	637	357.8	389.5	470.1	175.8	418	246.7	269.2	120.7	140.7	120.2
Ta	0.91	0.87	0.88	0.83	1.48	0.89	0.94	1.02	1.49	1.34	1.52
Tb	0.51	0.47	0.41	0.36	0.56	0.46	0.53	0.5	0.68	0.47	0.59
Th	8.91	8.64	7.57	6.89	10.88	7.27	11.66	12.29	16.69	14.73	16.39
Ti	3441	3361	3532	3199	3612	3378	2679	2444	2227	2061	1980
Tm	0.35	0.3	0.29	0.26	0.4	0.3	0.38	0.38	0.51	0.39	0.42
U	2.4	2	1.9	1.9	3.1	2.5	3.2	3	4.2	3	3.2
V	65	62	70	69	43	71	38	33	22	21	20
Y	16.3	14.7	13.4	11.4	18.1	13	15.1	14.1	23.8	15.5	18.4
Yb	1.7	1.6	1.5	1.2	2.2	1.4	2	2	2.8	2.1	2.2
Zn	68	62	55	44	150	39	58	37	101	77	132
Zr	74	58	61	49	58	63	105	96	69	117	64

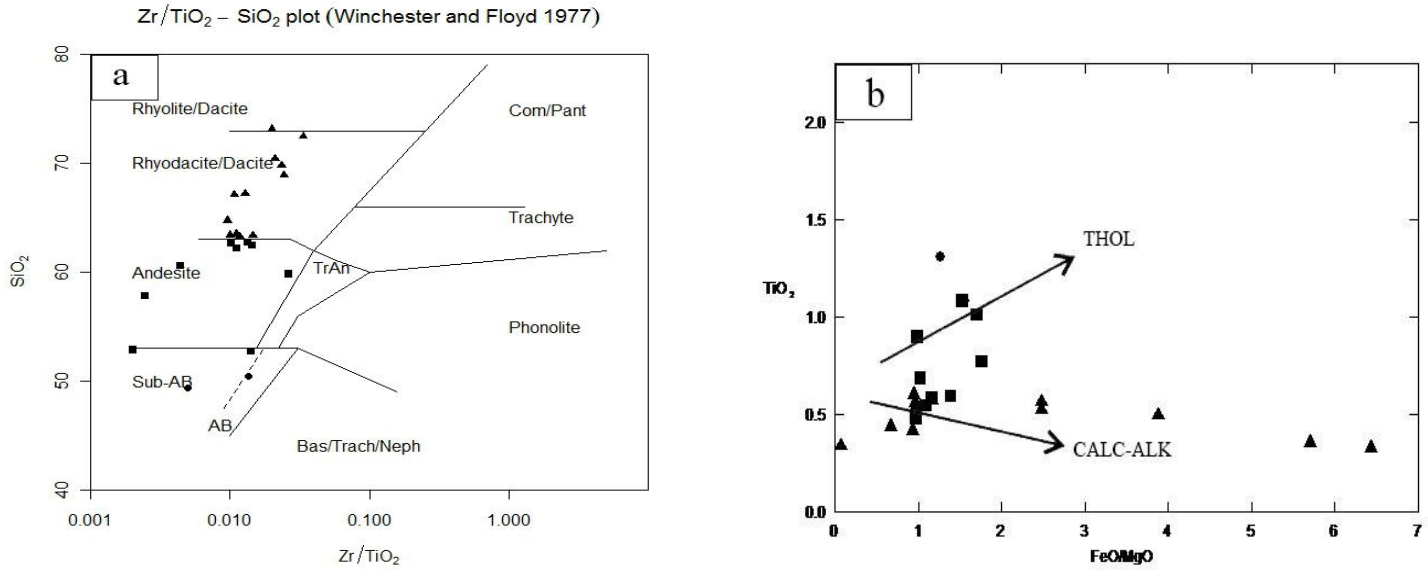

Figure 3- (a) The samples plotted based on their SiO2 versus Zr/TiO2 (Winchester, 1997) (b) the diagram of TiO2 versus FeO*/MgO [Thol and Calc-alk vectors have been cited from (●: basaltic samples; ■: intermediate samples; ▲: acidic samples)

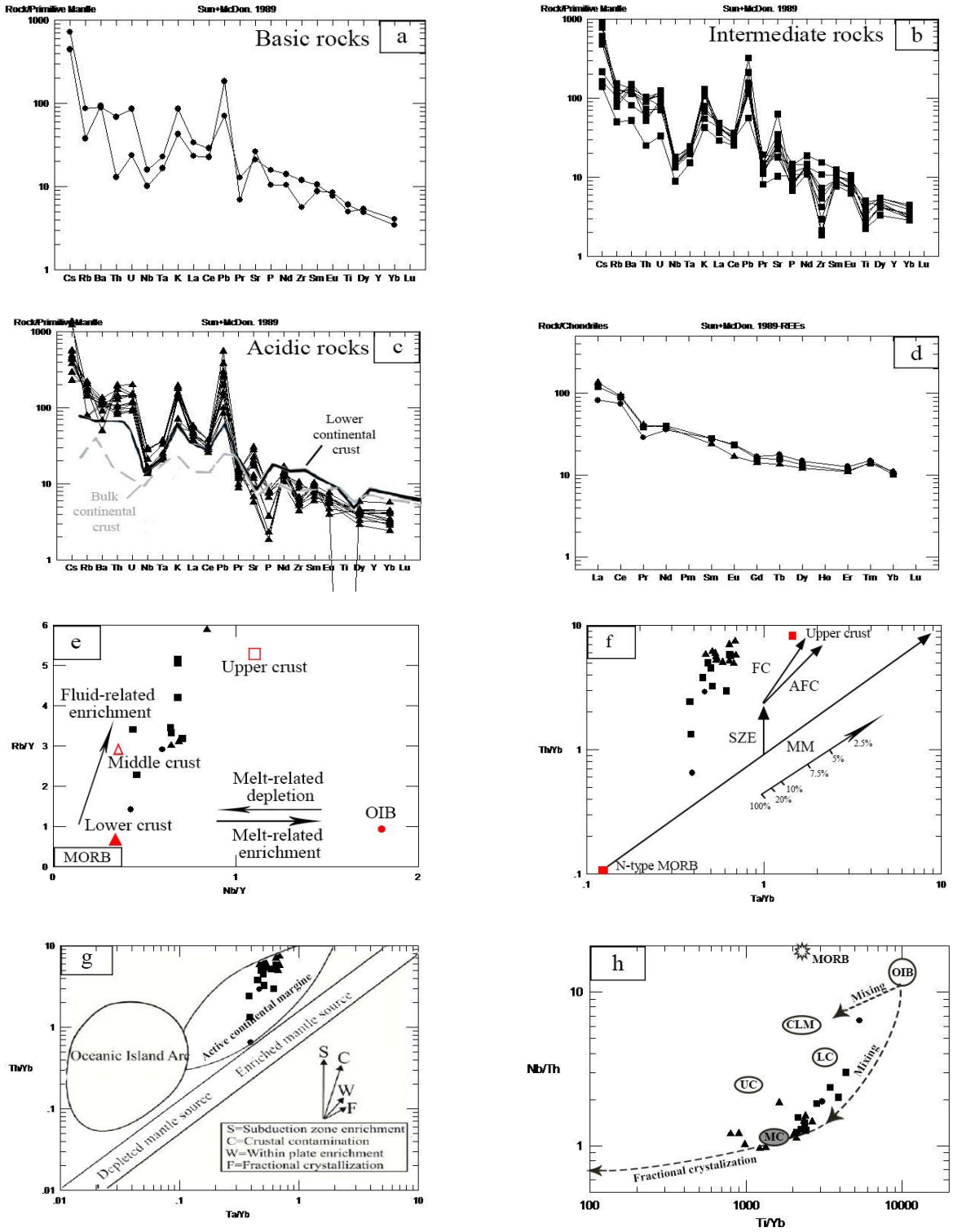

Figure 5- (a,b) multi elements pattern diagrams for normalized incompatible elements with the primary mantle for basic and intermediate rocks of the region, (c) a pattern for comparing REE normalized by primary mantle and crust for acidic samples (d) average REEs normalized by chondrite (e) Nb/Y versus Rb/Y (OIB from and lower and middle crust from) (f) Th/Yb versus Ta/Yb (MM: Inter-plate Metasomatic Mantle; SZE: Subduction Zone (FC and AFC (Fractional crystallization with assimilation) (g) Th/Yb versus Ta/Yb; (h) Nb/Th versus Ti/Yb (LC: Lower Mafic Crust;

MC: Medium Crust, CLM: Continental Lithospheric Mantle, UC: Upper Crust (●: basaltic samples; ■: intermediate samples; ▲: acidic samples)

Conclusion

A rhythmic lava layering is seen in the field trip where basic lava is placed in bottom parts and acidic lava is place in the upper parts; therefore, a magma chamber must have been responsible for the melting process.
Based on microscopic studies, the fractional crystallization can be well detected. Olivine basalt magma which has Olivine phenocryst has the least rate of fractional crystallization in the region. Olivine has been separated from the magma and consequently the amount of plagioclase and pyroxene has increased in the andesite basalt samples. As the fractional crystallization develops, the ratio of pyroxene phenocrysts to plagioclase has decreased and as water came to the magma composition, amphibole was appeared which is usually observed in pyroxene andesite rock units. Pyroxene phenocrysts have been crystalized in a late stages of fractional crystallization and quartz crystals are usually appeared in trachyandesite, dacite and rhyolite. Some evidence reveals an imbalance of primary magma as well as a quick process of becoming stone (from lave to stone). This evidence can prove the magma evaluation like magma mixing and magma contamination in the region. Based on the geochemical evidence, the magma is sub-alkaline to tholeiitic type.

Changes in major oxides and REEs show the rule of fractionation processes, different steps of partial melting and fractional crystallization of magma, heterogeneous mantle source, magma contamination of the source magma and assimilation with crustal rocks, mixing with acidic magma during the magma evaluation. The pattern of elements trend follows the continental crust trend. The source magma was influenced by fractional crystallization as well as FC and AFC processes. The magma was also contaminated and mixed with upper, middle and lower continental crusts. Therefore, the studied rocks are far away from their magma source in a geochemical point of view.

References

Abedian, N., Shahin, E., Alipour, M., 2009, Systematic Geochemical Exploration of Abhar's 1: 100000 Sheet, General Geological Project, Geochemical Project, Geological Survey of Iran.
Alavi, M., 1996, Tectonostratigraphic synthesis and structural style of the Alborz Mountain system in northern Iran. Geodynamic 21: 1-33.
Amini, B., 2000, 1/100000 Scaled Map of Taroom. Geological Survey of Iran.
Cai, Y., Wang, Y., Cawood, P.A., Fan, W., Liu., H., Xing, X., Zhang, Y., 2014, Neoproterozoicsubduction along the Ailaoshan zone, South China: Geochronological and geochemical evidence from amphibolite, Precambrian Research, 245, 13–28.
Dostal, J., 2017, Rare Earth Element Deposits of Alkaline Igneous Rocks, 6,34,1-12.
Eftekharnejad, J., Stocklin, J., Zahedi, M., Hajian, J., Houshmandzadeh, A., Alavi, M., 1969, 1/2500000 Scaled Map of Zanjan, Geological Survey of Iran.
Feigenson, M.D., Patino, L.C., Carr, M.J., 1996, Constraints on partial melting imposed by rare earth element variations in Mauna Kea basalts. J. Geophys. Res. 101, 11815–11829.
GhotbTahriri, F., Arian, M.A., Haghnazar, Sh., Pourkermani, M., 2017, Petrology of Sirdan volcanic rocks in Alborz Mountains, northern Iran, RevistaPublicando, Vol. 5. No. 14 (2), 19p.
Hofmann, A.W., Jochum, K.P., 1996, Source characteristics derived from very incompatible trace elements in Mauna Loa and Mauna Kea basalts, Hawaii Scientific Drilling Project. J. Geophys. Res. 101, 11831–11839.
Kamali, A.A., Moayyed, M., Jahangiri, A., Amel, N., Pirooj, H., Ameri, A., 2011, The petrography and geochemistry of volcanic rocks of Ghaflankuh, Myaneh (NW Iran), Petrology, 2nd Year, No. 6, 97-115.
Kepezhinskas, P., Defant, M.J., Drummond, M.S., 1996, Progressive enrichment ofisland arc mantle by melt-peridotite interaction inferred from Kamchatka xeno-liths. GeochimicaetCosmochimicaActa 60, 1217–1229.
Khalatbari, M., Akbari, M., Ghalamghash, J., 2016, Geology, Petrology and Magmatic evolutions of Eocene Volcanic Rocks in the area of Aqdagh, northeast Abhar, Journal of ScienceKharazmiUniversity, Vol, 2, No, 1, 33-60.
Khalifa, I.H., El-Bialy, M.Z., Hassan, D.M., 2011, Petrologic and geochemical characterization and mineralization of the metavolcanic rocks of the Heib Formation, Kid Metamorphic Complex,

Sinai, Egypt, Geoscience Frontiers, 2(3), 385-402.
Kheirkhah, M., 2013, New investigation on petrogenesis and age dating of quaternary basic lavas in northwest iran, to compare with source centers in turkish-iranian plateau, Scientific Quarterly Journal, Geosciences, Vol, 22, No,88, 205-218.
Koyaguchi, T., and Blake, L., 1991, Origin of mafic enclaves: Constraints on the magma mixing model from fluid dynamic experiments: Enclaves and granite petrology, Elsevier scientific pub. B.V., 415-429.
Krauskopf, K. B. and Bird, D. K., 1976, Introduction to geochemistry. Mcgraw-hill, Inc. 647p.
Li, D., He, D.F., Santosh, M., Tang, J.Y., 2014, Petrogenesis of Late Paleozoic volcanics from the Zhaheba depression, East Junggar: Insights into collisional event in an accretionary orogeny of Central Asia, Lithos 184–187, 167–193.
McDonough, W.F., 1990, Constraints on the composition of the continental lithospheric mantle, Earth planet. Sci. Lett., 101, 1-18.
Miyashiro, A., 1974, Volcanic rock series in Island arcs and active continental margins. Am. J. Sci. 274, 321-355.
Moayyed, M., 1991, Petrologic Investigations of Volcano-Plutonic Tertiary belt of Western Alborz- Azarbaijan with a Special View on Hashtjin Area, Ph.D. in geology Tabriz University, pp. 94-125.
Nabavi, M.H., 1976, An introduction to the geology of Iran. Geological Survey of Iran, Tehran, 109 p. (in Persian).
Nazari, H., Salamati, R., 1998, 1/100000 Scaled Map of Rudbar. Geological Survey of Iran.
Pearce, J. A., 1983, Role of the subcontinental lithosphere in magma genesis at active continental margins. In: Hawkesworth C.J. and Norry M.J., (eds.), Continental basalts and mantle xenoliths. Shiva, nantwich, 230-249.
Pearce, J.A., Bender, J.F., De Long, S.E., Kidd, W.S. F., Low, P.J., Gunner, Y., Saroglu, F., Yilmaz, Y., Moorbath, S., and Mithchell, J.G.,1990, Genesis of collision volcanism in eastern Anatolia, Turkey, J. Volc. Geotherm. Res, 44, 189–229.
Peyrowan, H.R., 2002, Geochemical study of hydrothermal alteration zones of magmatic rocks of Tarom area and its environmental effects, Doctoral dissertation of Geology (Ph.D), Islamic Azad University, Science and Research Branch.
Rudnick, R.L, Fountain, D.M., 1995, Nature and composition of the continental crust: a lower crustal perspective. Rev. Geophys. 33(3), 267–309.
Rudnick, R.L., Gao, S., 2003, The composition of the continental crust. In: Rudnick, R.L. (Ed.), The Crust. In: Holland, H.D., Turekian, K.K., (Eds.), Treatise on Geochemistry, vol. 3. Elsevier-Pergammon, Oxford. 64 pp.
Shelly, D., 1993, Igneous and metamorphic rocks under the microscope, Chapman and Hall, 405 pp.
Sun, S.S., and McDonough, W.F., 1989, Magmatism in the oceanic basalts (A.D. Saunders and M.J.Norry, Her ausgeber). Geological Society London Special Publications, 42, 313-345.
Taylor, S.R., and McLennan, S.M., 1985, The continental crust: it's composition and evolution. Blackwell, Oxford, England, 312 p.
Thomas, N., and Tait, S.R., 1997, Dimensions of magmatic inclusions as a constraint on the physical mechanism of mixing, Jour. Volcanol. Geotherm. Res., 75: 167-178.
Wilshire, H. G., McGuire, A. V., Noller, J. S., and Turrin, B. D., 1991, Petrology of lower crustal and upper mantle xenoliths from the Cima, Volcanic Field, California, J. Petrol., 32: 169-200.
Winchester, J.A, and Floyd, P.A., 1977, Geochemical discrimination of different magma series and their differentiation product using immobile elements. Chemical Geology 20: 325-343.
Winter, J.D., 2001, An introduction to igneous and metamorphic petrology, Prentice- hall inc. upper Saddle River, New Jersey. P 697.
Wright, T.L., and Helz, R.T., 1996, Differentiation and magma mixing on Kilauas east rift zone: Further look at the eruptions of 1955 and 1960, Bull. Volcanol, 57: 602-630.
Zarasvandi, A., Rezaei, M., Lentz, D., Pourkaseb, H., Karevani, M., 2015, The Kasian volcanic rocks, Khorramabad, Iran: Evidence for a Jurassic Intra-Oceanic island arc in Neo-Tethys ocean, IJST , 39A2: 165-178.
Zhao, J.H., and Zhou, M.F., 2007, Geochemistry of Neoproterozoic mafic introsions in the panzhihua district (Sichuan Province, SW China): Implication for subduction related metasomatism in the upper mantle. Precambrian Research. 152: 27-47.